An Experimental Investigation into the Influence of User State and Environment on Fading Characteristics in Wireless Body Area Networks at 2.45 GHz

Simon L. Cotton, *Member, IEEE,* and William G. Scanlon, *Member, IEEE*

***Abstract*—Using seven strategically placed, time-synchronized bodyworn receivers covering the head, upper front and back torso, and the limbs, we have investigated the effect of user state: *stationary* or *mobile* and local environment: *anechoic chamber*, *open office area* and *hallway* upon first and second order statistics for on-body fading channels. Three candidate models were considered: Nakagami, Rice and lognormal. Using maximum likelihood estimation and the Akaike information criterion it was established that the Nakagami-m distribution best described small-scale fading for the majority of on-body channels over all the measurement scenarios. When the user was stationary, Nakagami-m parameters were found to be much greater than 1, irrespective of local surroundings. For mobile channels, Nakagami-m parameters significantly decreased, with channels in the open office area and hallway experiencing the worst fading conditions.**

***Index Terms*—Bodyworn antennas, channel characterization, on-body propagation, wireless body area networks.**

I. Introduction

IT has long been established that the local environment plays an important role in the performance of radio communications systems. The experiments of Rappaport [1], Bultitude [2] and Saleh [3] are well known examples representative of the many investigations over the last few decades which have characterized radio propagation for non-bodyworn systems in a wide range of environments. When combined with complex propagation mechanisms such as diffraction, reflection and scattering, the nature of the local environment is responsible for diffusion of the transmitted wave into a continuum of partial waves with varying amplitude and phase resulting in spatial variations in the electromagnetic field strength observed at a receiver. With the advent of bodyworn communications, this traditional radio channel becomes more difficult to characterize due to the often stochastic (temporal) influences of the human body which, in turn, are largely determined by the user's state. Furthermore, because of the transitory nature of human life, the permutations of user state and local environment are almost limitless, rendering the development of a generic deterministic model for bodyworn radio systems impractical. An alternative approach, which circumvents this complexity, is to provide a statistical description of these channels for selected scenarios. Therefore, it is imperative that detailed radio propagation studies for stationary and mobile user states should be carried out in all environments where wearable systems will be expected to operate.

A wireless body area network (WBAN) is a particular type of wearable system where a number of radio devices form a self-contained network on the human body, with the emphasis upon communication across the body surface. There are a number of different IEEE standards which may be used as a basis for data communications in WBANs including the IEEE 802.15.1 [4] and 802.15.4 [5] standards, both of which incorporate spectrum allocations in the 2.45 GHz band investigated in this study. The rationale behind the IEEE 802.15.4 standard is to provide a low power, low data rate wireless interface between radio devices, with obvious relevance to a number of specialized WBAN applications such as patient healthcare [6] where wireless sensors may be used to monitor post surgery recovery, or the surveillance of the chronically ill [7]. A limited amount of research relating to on-body propagation has appeared in the peer-reviewed literature. Fading characteristics within the European 868 MHz band have previously been investigated for bodyworn communications in both wireless personal area networking and WBAN applications [8], [9]. In [10], on-body path loss distribution was investigated for a stationary user in an anechoic chamber and laboratory environment. The authors report that the path loss distribution was well described by the lognormal distribution and that the human body is the dominating shadowing factor in wireless body area networks. Fort *et al* [11], [12] have investigated the use of UWB channels in on-body systems and developed practical models which may be used to evaluate their performance in WBANs. Through resampling they have been able to report some first order statistics for small-scale fading in an indoor environment while the user was stationary [11] and in the case of limited movements of the arms [12]. While there are a wide range of issues affecting on-body systems, in this paper we have focused solely on small-scale fading and the concentrated on reporting the effects of the user state and local environment.

The remainder of this paper is organized as follows. The measurement environments, on-body measurement system and experimental procedure are described in Section II. Section III presents first and second order statistics for on-body channels considering both user stationary and mobile scenarios in the anechoic chamber. In Section IV, we present statistics for

Manuscript received July 20, 2007; revised November 22, 2007; accepted January 16, 2008. The associate editor coordinating the review of this paper and approving it for publication was H. Xu.

The authors are with the School of Electronics, Electrical Eng. and Computer Science, Queen's University, Belfast, BT3 9DT, UK (e-mail: {simon.cotton, w.scanlon}@qub.ac.uk).

This work was supported in part by the U.K. Engineering and Physical Sciences Research Council (grant ref. EP/D053749/1).

Digital Object Identifier 10.1109/T-WC.2009.070788

the equivalent channels in the open office area and hallway and propose general Nakagami models which aim to describe overall fading in mobile WBANs. Section IV also includes a selection of simulated results obtained using Nakagami, Rice and lognormal waveform generators. Before concluding the paper with Section VI, we present a physical interpretation of the fading experienced in WBANs in Section V.

II. On-Body Measurements

Measurements were performed at the recently constructed three-story ECIT building at Queen's University, Belfast, UK. Three separate indoor environments were considered: anechoic chamber, open office area and hallway, which were all situated on the ground floor (Fig.1) and described in [9]. The bodyworn measurement system consisted of seven purposely developed, self-contained, ultra-low form factor 2.45 GHz data logging modules based around a Linear Technology LT5504 RF measuring receiver as extensively described in [13]. All units were directly fixed (no dielectric spacers or extended groundplanes) to a 3 mm thick, tight fitting polychloroprene / nylon contoured suit and neoprene hood to minimize spurious antenna-body separation effects. The receivers were positioned so that the radiating element of their integrated printed-F antenna (gain of 4.9 dBi, impedance bandwidth of 170 MHz) was pointing in a vertical direction, parallel to the user's body. The seven receiver locations, considered to be representative of a WBAN configuration, are shown in Fig.2. The transmitter (TX) used in each of set of experiments was a NovaSource G6 synthesized RF signal source (whose output was amplified using a Hittite HMC-455LP3 amplifier to ensure adequate dynamic range at each receiver, regardless of position) with a 2.0 dBi sleeve dipole antenna. The TX was mounted vertically at the test person's left waist (Fig.2) and configured to operate in continuous wave (CW) mode with an overall transmit power of $+22$dBm at 2.45GHz.

The bodyworn measurement system was worn by an adult male of mass 83 kg and height 1.72 m. For robustness, the on-body measurements consisted of two individual trials of each scenario. All three environments were unoccupied for the duration of each experiment. Initially, the user was instructed to stand motionless at position A in the anechoic chamber (Fig.1) with the RF source at his waist. All of the receiver units were activated to make synchronous measurements of the received signal (at a sampling rate of 256 Hz) and then after around 10s the TX was momentarily keyed off to allow a recognizable gap in the results. This process was repeated for the second trial. The same technique was applied for mobile measurements between AB within the chamber. Further stationary measurements were made at points C, for the open office area environment and E for hallway. Corresponding mobile measurements were conducted along paths CD and DE. A total of 227500 samples were collected. The shortest received signal envelope consisted of 2000 samples (7.8 s) and occurred for trial 1 of user stationary measurements in the hallway. The average straight line velocity for each of the mobile sessions was estimated to be approximately 1.0 ms^{-1}, based on distance and elapsed time for each trajectory.

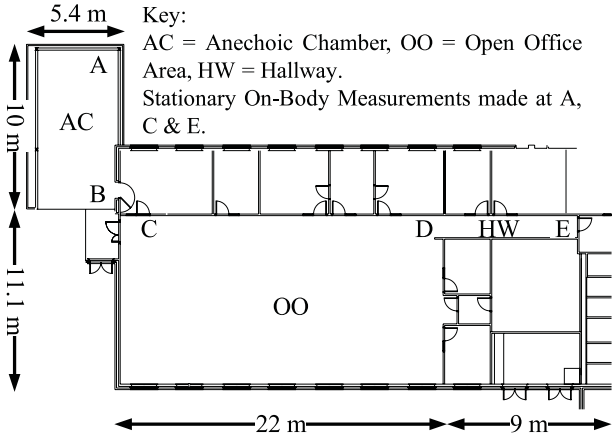

Fig. 1. Plan view of measurement locations showing key position markers (not to scale): anechoic chamber (54 m^2), open office area (244.2 m^2) and hallway (13.5 m^2).

Fig. 2. On-body transmitter (TX) and right-head (RH), left-head (LH), front-right-chest (FRC), front-left-chest (FLC), front-right-wrist (FRW), front-right-ankle (FRA) and back-right-chest (BRC) receiver positions.

III. Anechoic Chamber

Three probability distributions, all of which have been previously used to model fading channels which involve the human body, were considered: Nakagami [8], [9], Rice [9], [14] and lognormal [11], [12], [14]. Prior to the statistical analysis performed here, all measured received signal envelopes where normalized to their respective global medians. All distribution parameter estimates presented were obtained on a 95% confidence interval using the $\mathsf{mle}(\cdot)$ function available in the statistics toolbox of Matlab. Model selection in this paper is based upon the Akaike Information Criterion (*AIC*) [15]. Fort *et al.* [12] provide a comprehensive discussion of the *AIC*'s use and its limitations in the selection of fading models in on-body channels. In a similar manner to the analysis presented in [12] we use the second-order *AIC* often denoted AIC_c (equation (2) of [12]). It can be shown quite easily that independent likelihoods can be combined. We exploit this

property of maximum likelihood estimators to consider the outcome of more than one experiment in the calculation of the AIC_c.

Table I shows a summary of the AIC_c favored models for each scenario / environment. While the user was stationary in the reduced multipath conditions of the anechoic chamber, no clear pattern between a particular model and propagation path was observed. Unless otherwise stated, maximum calculated Akaike weights [12] for channels in the anechoic chamber, and indeed over the remaining scenarios / environments, were found to be equal to one providing strong evidence for the adoption of respective statistical fading models. In the user-stationary, anechoic chamber scenario, the median estimated Nakagami m parameter was m=41.87 with corresponding 1st and 3rd quartiles m=20.83 and m=52.40, respectively. As $m\rightarrow\infty$ the Nakagami pdf approaches a delta function (no fading) hence these channels are relatively deterministic. Respiratory related effects such as the displacement of antennas, varying antenna-body coupling and variations in body shape caused only minor changes in the channel. The measured fade margin (observed from the raw data) in these channels and for similar channels under stationary user conditions in other environments were nearly always within $\pm$3 dB of the median signal level. This suggests that the analysis of these channels using traditional fading statistics may not be entirely appropriate, except for the most marginal of systems. For these reasons, and due to space limitations, we limit the subsequent discussion of user stationary channels.

While the user was mobile in the anechoic chamber, the number of channels which experienced Nakagami fading increased (Table I). This trend was also repeated over the other two environments considered. Because of the Nakagami distribution's predominance in user mobile on-body channels, and its ability to approximate the Rice pdf [16], we concentrate on this fading model to explain the on-body propagation channels in this WBAN study. Table I also presents the ML estimated Nakagami parameters and maximum Doppler frequency [9] for all user mobile channels in each of the three test environments. When the user became mobile, the observed Nakagami-m parameters were vastly reduced compared to user stationary scenarios showing that motion has a major effect on channel statistics. The variation in ML estimated Nakagami coefficients was observed to be greatest for this environment (anechoic) ranging from m=1.31 for the front-right-wrist to m=13.7 for the front-right-chest. Bodyworn receivers positioned at the front-right-wrist and front-right-ankle experienced the greatest degree of fading as m values here were lower than for other body locations. Because both of these receivers are placed on the users limbs, they are likely to experience highly changing channel conditions, confirmed by the maximum Doppler frequency for these devices (f_m>5.20 Hz), with only the right-head receiver experiencing greater channel variation (f_m=8.36 Hz). Fading envelopes observed on either side of the user's head were found to have first order statistics which were very similar, although for receivers on the user's front chest, a significant difference in ML estimated Nakagami-m parameters was observed (Table I).

Two second order statistics which are of great importance in the design of mobile radio systems and analysis of their performance [17] are the level crossing rate (LCR), which is the number of times a signal crosses a threshold level in a positive (or negative) going direction, and the average fade duration (AFD), which is the total amount of time spent below the same threshold level. Among their uses is the design of error correcting codes, optimization of interleaver size and system throughput analysis as well as channel modeling. Fig.3 shows an example of the theoretical Nakagami [18], Rice [19] and lognormal LCRs [20] and AFDs fitted to experimental second order data, calculated in steps of 0.5 dB in the threshold range -30 to 30 dB, for the back-right-chest positioned receiver. The empirical LCR and AFD here, and in the illustrated examples which follow, are plotted on a log-log scale to expand the tail of the distributions to ensure that the fitted models provide an adequate description of the data at the lowest fading levels which are known to determine the bit error rate in marginal systems. It can be seen quite clearly from both sets of plots that the Nakagami LCRs and AFDs of [18] provide a good fit.

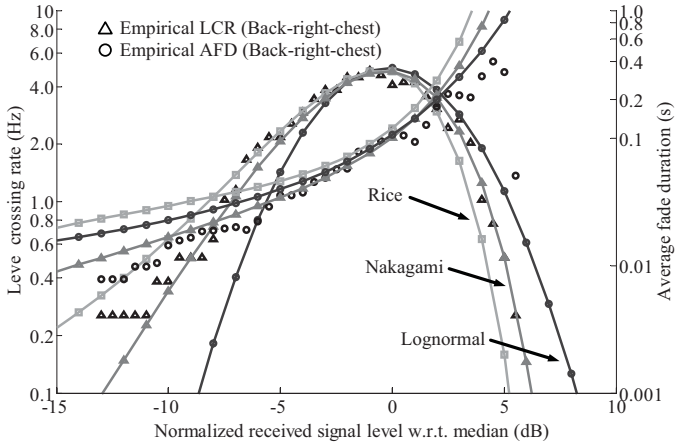

Fig. 3. Empirical and theoretical LCR and AFD functions for the back-right-chest receiver while the user was mobile in the anechoic chamber. MLE predicted parameters for the models are; Nakagami m=2.46, Ω=1.18, Rice A=0.97, s=0.35 and lognormal μ=$-$0.02, σ=0.35. Note that distinct from the second order statistics presented later, the LCR and AFD are not normalized to the maximum Doppler frequency.

IV. Open Office Area and Hallway

A. Open Office Area

AIC_c indices calculated for the open office area again favored the Nakagami distribution. As expected, due to increased multipath contribution from the local surroundings, estimated Nakagami-m parameters for a user stationary state in the open office area were lower than corresponding measurements in the anechoic chamber. The median m value here was 16.73 with 1st and 3rd quartiles of m=16.05 and m=67.36, respectively. It should be noted that although the Nakagami-m values were less in the open office area than corresponding measurements in the anechoic chamber, both sets of m parameters were still $\gg 1$.

With the exception of the front-right-wrist and front-right-ankle, when the user became mobile within the multipath conditions of the open office area, the remaining on-body channels had m parameters which were significantly reduced

TABLE I
ML ESTIMATED NAKAGAMI PARAMETERS AND MAXIMUM DOPPLER FREQUENCY FOR ALL MOBILE WBAN CHANNELS ALONGSIDE SUMMARY OF AIC_c FAVORED MODEL FOR EACH SCENARIO / ENVIRONMENT. KEY: STATIONARY (STAT), MOBILE (MOB)

	Anechoic Chamber (AC)			Open Office (OO)			Hallway (HW)			AIC_c favored model			
RX Position	m	Ω	f_m (Hz)	m	Ω	f_m (Hz)	m	Ω	f_m (Hz)	Environ.	Nakagami	Rice	Lognormal
Right-head	2.39	1.10	8.36	1.35	1.29	12.4	1.27	1.28	11.2	AC Stat	3/7	2/7	2/7
Left-head	2.55	0.92	3.33	1.22	1.40	8.71	1.16	1.54	8.79	AC Mob	4/7	2/7	1/7
Front-right-chest	13.7	0.95	2.92	1.39	1.15	10.8	1.33	1.32	9.67	OO Stat	4/7	2/7	1/7
Front-left-chest	8.99	1.08	2.67	3.61	1.18	9.18	2.64	1.22	8.61	OO Mob	4/7	1/7	2/7
Front-right-wrist	1.31	1.35	7.69	1.49	1.17	13.2	1.57	1.17	13.4	HW Stat	3/7	2/7	2/7
Front-right-ankle	1.33	1.26	5.20	1.11	1.39	8.24	1.25	1.46	8.79	HW Mob	5/7	1/7	1/7
Back-right-chest	2.46	1.18	4.70	1.52	1.22	9.62	1.72	1.07	9.38	Overall	55%	24%	21%

compared to the anechoic chamber (Table I). Interestingly, Nakagami-m parameters for receivers placed on the limbs appeared to be largely unperturbed by change of environment, although still remaining greater than one, suggesting that even in these highly dynamic channels (in terms of movement), a dominant signal contribution still exists. As the ML estimated Nakagami-m parameters in the open office area were within the range $1.11<m<3.61$, a general Nakagami distribution was fitted to an amalgamated vector of the normalized deviations for all on-body channels. Parameter estimates for this model were obtained using ML estimation. A similar process was used to obtain general models for the Rice and lognormal distributions for comparison. The general model parameters were; Nakagami, m=1.44, Ω=1.27, Rice, A=0.86, s=0.51 and lognormal, $\mu=-0.07$, σ=0.49.

Generic models describing second order statistics for all on-body channels are shown in Fig.4. Here, the individual LCRs and AFDs for these plots are normalized to the maximum Doppler frequency. Empirical normalized crossing rates for the front-left-chest chest receiver are observed to be lowest below the median signal level, presumably due to the shorter signal propagation path found in this channel. For the remaining on-body channels, the normalized LCRs were found to be largely similar, exhibiting comparable crossing rates above and below the median signal level and justifying the use of a general model to describe the data. The Nakagami LCR of (equation (9) of [18]) with the exception of the front-left-chest, receiver provides a good description of all channels until -20 dB below the median signal level. It should be noted from the empirical CDF (not shown) that fades below this level accounted for less than 0.1 % of all signal levels considered. If greater accuracy is required, or in the case of the front-left-chest, the exact Nakagami parameter estimates (Table I) should be used instead. Fig.5 shows an example of simulated second order statistics generated using the rank matching approach proposed in [21], for the right-head on-body position while the user was mobile in the open office area. The simulated Nakagami, Rice and lognormal envelopes each consisted of 4000 samples to match the size of the measured channel. In both cases, simulated Nakagami statistics were found to closely match measured results.

B. Hallway

The Nakagami distribution was also found to account for the majority of user stationary models in this environment (Table I). The median Nakagami-m parameter in the hallway, m=21.75, was found to be greater than that of the open office area, although again, $m \gg 1$. ML estimated Nakagami-m parameters for mobile channels in the hallway environment were found to be comparable to those observed in the open office area (Table I), with the top four positioned receivers experiencing a slight decrease in predicted m-values possibly due to the reduced dimensions of the hallway environment increasing the multipath contribution at this level. The overall range here was reduced to $1.16<m<2.64$, meaning that the general fitted models provided an excellent fit to all measured data. ML general models for the hallway were found to have parameters: Nakagami (m=1.43, Ω=1.30), Rice (A=0.85, s=0.54) and lognormal ($\mu=-0.07$, σ=0.49). As the parameter estimates for the general model for the hallway were very similar to those for the open office area, this suggests that it may be possible to use one generic model for both environments, when considering on-body propagation paths in which bodyworn receivers are not in the immediate vicinity of the transmitter.

V. A PHYSICAL INTERPRETATION OF FADING IN WBANS

Based on the fading models considered, and results presented above, we provide an interpretation of the propagation of electromagnetic (EM) waves in wireless body area networks. When viewed from an EM perspective, at 2.45 GHz the human body acts an inhomogeneous interfering object, with dielectric properties which can vary significantly between different on-body locations and indeed from person to person. The electromagnetic problem can be viewed as being composed of two separable factors, firstly the effect of the body upon the antenna such as bulk power absorption (efficiency), time-varying resonant frequency shifts and radiation pattern fragmentation [22], and secondly the combination of transmission path, user state and environment (i.e., propagation), both of which are related to the non-uniform make-up of the human body. For example, with an on-body receiver placed at the left-chest of an adult male such as that used in this study, the primary dielectric structure is predominantly muscle, with dielectric constant ϵ_r=53.57 and conductivity σ=1.81 Sm^{-1} at 2.45 GHz [23]. However, for a receiver placed only a short distance away (typically < 0.2 m) at the left side of the human head, the skull is prominent with a significantly different parameters (ϵ_r=14.97, σ=0.60 Sm^{-1}). For the experiments conducted in this study, no direct line of sight path is available due to the location of the transmitter at the side of the human body and the low form factor of the receiver design. At this frequency, it is expected that the primary signal contribution arrives via creeping (trapped surface) wave contribution along

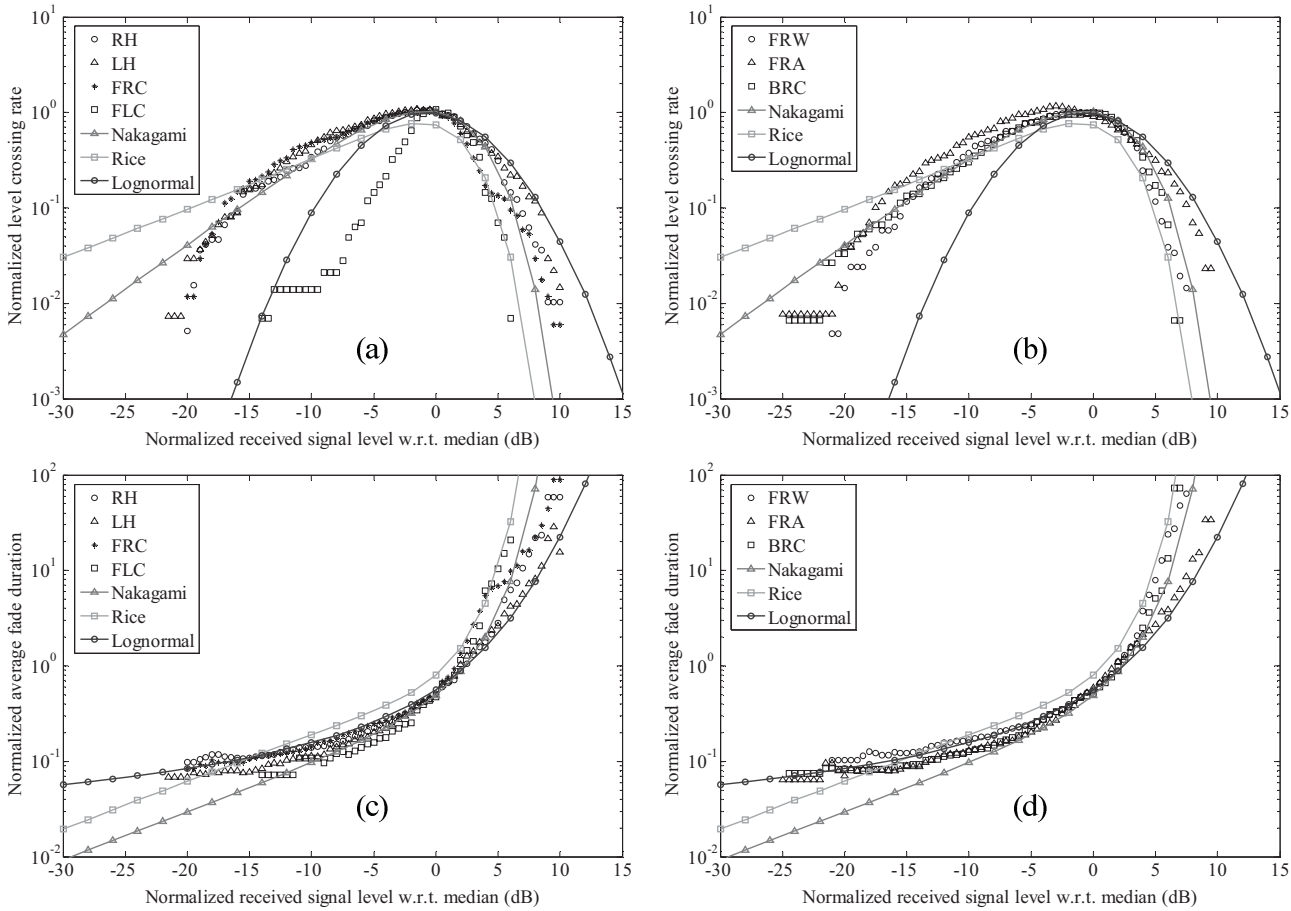

Fig. 4. Normalized empirical and theoretical LCR and AFD functions for (a) & (c) right-head (RH), left-head (LH), front-right-chest (FRC), front-left-chest (FLC) and (b) & (d) front-right-wrist (FRW), front-right-ankle (FRA), back-right-chest (BRC) receivers while the user was mobile in the open office area. General model parameters are; Nakagami m=1.44, Ω=1.27, Rice A=0.86, s=0.51 and lognormal μ=−0.07, σ=0.49.

the perimeter of the human body [24]. As the creeping wave extends across the surface of the human body it will become perturbed as it interacts with the irregular physical body characteristics and inhomogeneous dielectric structures encountered. Consequently, reflection, diffraction, scattering and absorption, will become responsible in varying degrees, depending upon user state and transmission path length, for creating a spatially distributed on-body EM field with random amplitude and phase. When the user is stationary and the only variation in the on-body channel is due to respiration, the diffuse contribution from these mechanisms is negligible compared to the dominant creeping wave component, a view which is supported by the high median Nakagami-m parameter obtained for the anechoic chamber (m=41.87). In addition, a change in local environment conditions from anechoic to multipath causes only a moderate increase in the diffuse signal contribution and channels are still largely composed of a dominant wave component (median m value always $>$16.73 for open office area and hallway).

When the user becomes mobile, the time-varying on-body EM field pattern now becomes interrupted at a much faster rate due to the user's movement. The instantaneous field strength experienced at each location on the user's body is now composed of the superposition of waves resulting from diffraction around the side of the user's body, creeping wave components which may now become periodically disrupted and, most importantly, increased scattered and reflected contributions due to the more frequent changes in geometrical body shape and posture. Under this rationalization of on-body propagation, it would be expected that with increasing transmitter-receiver separation distance, a higher diffuse signal contribution from on-body scatterers which reside in the transmission path would occur. A special exception here is for the case of receivers placed on the limbs, which under most circumstances should automatically experience the greatest degree of scattering due to the highly changeable channel conditions at these positions. If we initially exclude the effect of the immediate environment, these assertions can be shown to hold. While mobile in the anechoic chamber, receivers positioned at the user's front chest experienced high Nakagami-m factors (m>8.89). As the EM field spreads further across the user's body, scattering due to physical irregularities and changing surface dielectrics act to produce a greater number of partial waves each with random amplitude and phase which contribute to the final received signal level. This is confirmed by the significantly lower m parameters observed at positions such as the right-head (m=2.39), left-head (m=2.55) and back-right-chest (m=2.46). The lowest overall m-parameters in the anechoic chamber were indeed found on the user's limbs; front-right-wrist, m=1.31, front-right-ankle, m=1.33.

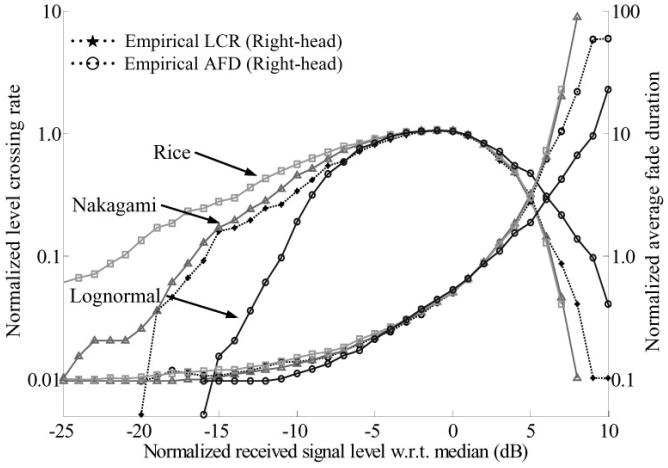

Fig. 5. Normalized empirical and simulated LCR and AFD functions for the right-head receiver while the user was mobile in the open office area. MLE predicted parameters for the models are; Nakagami m=1.35, Ω=1.29, Rice A=0.85, s=0.53 and lognormal μ=−0.08, σ=0.52.

Up until this point, we have ignored the effect of the immediate environment upon the fading characteristics observed in mobile WBANs. While the same basic mechanisms for propagation on and around the body are expected to hold, interfering objects such as complex building structures, furniture and pedestrians in the local surroundings are expected to significantly affect on-body systems. As discussed above, the spatial EM field formed on and around the stationary human body is now moderately affected by complex building structures. However, when the user becomes mobile, the random scattered component generated by the body is further enhanced by the environmental multipath which ordinarily (in the anechoic chamber) would have been lost. This observation is immediately recognizable from Table I where all receiver positions, with the exception the front-right-wrist, had ML estimated Nakagami-m parameters which were reduced for both the open office area and hallway compared to the anechoic chamber.

VI. Conclusion

In this paper, we have focused solely on the signal fading experienced by a wireless body area network consisting of a number of strategically placed bodyworn receivers operating at 2.45 GHz for two user states in three different physical environments. Based on time-synchronous measurements, it has been established that user state and local environment play an important role in the determination of on-body propagation characteristics. When the user is stationary, very little fading is observed in on-body channels and Nakagami-m parameters are always $\gg 1$. For a mobile user, the Nakagami-m distribution was found to account for 62% of all channels analyzed over the three environments. Compared to user stationary measurements the m parameter was found to significantly decrease providing evidence that motion acts to increase the diffuse on-body component experienced by bodyworn receivers. On-body fading was also found to increase when the user moved from anechoic to multipath conditions, although limb mounted receivers experienced fading which was comparable in all three environments. Maximum likelihood estimated Nakagami model coefficients have been presented for all measured channels when the user was mobile. Using these coefficients, on-body channels may be approximately reproduced using available Nakagami waveform generators. Second order statistics have also been presented for a selection of on-body channels and mostly found to be in good agreement with Nakagami. Finally, general models for the Nakagami, Rice and lognormal small-scale fading for on-body channels while the user was mobile in the open office area and hallway have been provided and shown to provide a good description for measured channels.

Acknowledgment

The authors would like to acknowledge Mr. Thomas Cotton for his help with the construction of the bodyworn measurement system. The authors would also like to extend their gratitude to Hittite, Linear Technology, Taconic and ZComm for their generosity and support throughout this work.

References

[1] T. Rappaport, "UHF fading in factories," *IEEE J. Select. Areas Commun.*, vol. 7, pp. 40–48, Jan. 1989.

[2] R. J. C. Bultitude, "Measurement, characterization and modeling of indoor 800/900 MHz radio channels for digital communications," *IEEE Commun. Mag.*, vol. 25, pp. 5–12, June 1987.

[3] A. Saleh and R. Valenzuela, "A statistical model for indoor multipath propagation," *IEEE J. Select. Areas Commun.*, vol. 5, pp. 128–137, Feb. 1987.

[4] IEEE Std. 802.15.1-2002, "IEEE Standard for Information Technology, Telecommunications and Information Exchange Between Systems, Local and Metropolitan Area Networks: Specific Requirements, Part 15.1: Wireless Medium Access Control (MAC) and Physical Layer (PHY) Specifications for Wireless Personal Area Networks," 2002.

[5] IEEE Standards for Information Technology Part 15.4: Wireless Medium Access Control (MAC) and Physical Layer (PHY) Specifications for Low-Rate Wireless Personal Area Networks (LR-WPANs), IEEE Std. 802.15.4-2003, 2003.

[6] U. Varshney and S. Sneha, "Patient monitoring using adhoc wireless networks: Reliability and power management," *IEEE Commun. Mag.*, vol. 44, pp. 49–55, Apr. 2006.

[7] N. Herscovici, C. Christodoulou, E. Kyriacou, M. S. Pattichis, C. S. Pattichis, A. Panayides, and A. Pitsillides, "m-health e-emergency systems: current status and future directions," *IEEE Antennas Propagat. Mag.*, vol. 49, pp. 216–231, Feb. 2007.

[8] S. L. Cotton and W. G. Scanlon, "A statistical analysis of indoor multipath fading for a narrowband wireless body area network," in *17th IEEE Intl. Symp. Personal, Indoor & Mobile Radio Comms. (PIMRC)*, pp. 1–5, Helsinki, Finland, Sept. 2006.

[9] S. L. Cotton and W. G. Scanlon, "Characterization and modeling of the indoor radio channel at 868 MHz for a mobile bodyworn wireless personal area network," *IEEE Antennas Wireless Propag. Lett.*, vol. 6, pp. 51–55, 2007.

[10] A. Alomainy, Y. Hao, A. Owadally, C. G. Parini, Y. Nechayev, C. C. Constantinou, and P. S. Hall, "Statistical analysis and performance evaluation for on-body radio propagation with microstrip patch antennas," *IEEE Trans. Antennas Propag.*, vol. 55, pp. 245–248, Jan. 2007.

[11] A. Fort, J. Ryckaert, C. Desset, P. De Doncker, P. Wambacq, and L. Van Biesen, "Ultra-wideband channel model for communication around the human body," *IEEE J. Select. Areas Commun.*, vol. 24, pp. 927–933, Apr. 2006.

[12] A. Fort, C. Desset, P. De Doncker, P. Wambacq, and L. Van Biesen, "An ultra-wideband body area propagation channel Model-from statistics to implementation," *IEEE Trans. Microw. Theory Tech.*, vol. 54, pp. 1820–1826, June 2006.

[13] S. L. Cotton and W. G. Scanlon, "The κ–μ distribution applied to the analysis of fading in body to body communications channels for fire and rescue personnel," *IEEE Antennas and Wireless Propagation Lett.*, vol. 7, pp. 66–69, 2008.

[14] S. L. Cotton and W. G. Scanlon, "Indoor channel characterisation for a wearable antenna array at 868 MHz," in *Proc. IEEE Wireless Commun. & Networking Conf.*, pp. 1783–1788, Apr. 2006.

[15] H. Akaike, "A new look at the statistical model identification," *IEEE Trans. Autom. Control*, vol. 19, pp. 716–723, Dec. 1974.

[16] M. Nakagami, "The m-distribution: a general formula of intensity distribution of rapid fading," in *Statistical Methods in Radio Wave Propagation*. New York: Pergamon, pp. 3–36, 1960.

[17] N. Youssef, T. Munakata, and M. Takeda, "Fade statistics in Nakagami fading environments," in *Proc. IEEE 4th Intl. Symp. Spread Spectrum Tech. & Appl.*, vol. 3, pp. 1244–1247, 1996.

[18] M. D. Yacoub, J. E. V. Bautistu, and L. Guerra de Rezende Guedes, "On higher order statistics of the Nakagami-m distribution," *IEEE Trans. Veh. Technol.*, vol. 48, pp. 790–794, May 1999.

[19] K. I. Ziri-Castro, W. G. Scanlon, and N. E. Evans, "Measured pedestrian movement and bodyworn terminal effects for the indoor channel at 5.2 GHz," *Europ. Trans. Telecommun.*, vol. 14, pp. 529–538, Jan. 2004.

[20] S. L. Cotton and W. G. Scanlon, "Higher order statistics for lognormal small-scale fading in mobile radio channels," *IEEE Antennas Wireless Propag. Lett.*, vol. 6, pp. 540–543, 2007.

[21] J. C. S. S. Filho, M. D. Yacoub, and G. Fraidenraich, "A simple accurate method for generating autocorrelated Nakagami-m envelope sequences," *IEEE Commun. Lett.*, vol. 11, pp. 231–233, Mar. 2007.

[22] W. G. Scanlon and N. E. Evans, "Numerical analysis of bodyworn UHF antenna systems," *IEE Electronics & Commun. Eng. J.*, vol. 13, no. 2, pp. 53–64, Apr. 2001.

[23] C. Gabriel, "4-Cole-Cole analysis on compilation of the dielectric properties of body tissues at RF and microwave frequencies," *Brooks Air Force Technical Report AL/OE-TR-1996-0037*, 1996.

[24] J. Ryckaert, P. Doncker, R. Meys, A. de Le Hoye, and S. Donnay, "Channel model for wireless communication around human body," *Electron. Lett.*, vol. 40, no. 9, pp. 543–544, Apr. 2004.